



Martian Thermospheric Response to an X8.2 Solar Flare on September 10, 2017 as seen by MAVEN/IUVS

S. K. Jain¹, J. Deighan¹, N. M. Schneider¹, A. I. F. Stewart¹, J. S. Evans²,

E. M. B. Thiemann¹, M. S. Chaffin¹, M. Crismani¹, M. H. Stevens³,

M. K. Elrod⁴, A. Stiepen⁵, W. E. McClintock¹, D. Y. Lo⁶, J. T. Clarke⁷, F. G.

Eparvier¹, F. Lefèvre⁸, F. Montmessin⁸, G. M. Holsclaw¹, P. C. Chamberlin¹,

B. M. Jakosky¹

S. K. Jain, Sonal.Jain@lasp.colorado.edu

¹Laboratory for Atmosphere and Space
Physics, University of Colorado Boulder,
Boulder, Colorado, USA

²Computational Physics, Inc., Springfield,
Virginia, USA

³Naval Research Laboratory, Washington,
District of Columbia, USA

This article has been accepted for publication and undergone full peer review but has not been through the copyediting, typesetting, pagination and proofreading process, which may lead to differences between this version and the Version of Record. Please cite this article as doi: 10.1029/2018GL077731

We report the response of the Martian upper atmosphere to a strong X-class flare on September 10, 2017 as observed by the Imaging Ultraviolet Spectrograph (IUVS) instrument aboard the Mars Atmosphere Volatile Evolution (MAVEN) mission. The solar flare peaked at 16:24 hrs UT and IUVS dayglow observations were taken about an hour after the flare peak. Retrieved temperatures from IUVS dayglow observations show a significant increase during the flare orbit, with a mean value of ~ 270 K and a maximum value of ~ 310 K. The retrieved temperatures during the flare orbit also show a strong latitudinal gradient, indicating that the flare induced heating is limited between low- and mid-latitudes. During this event IUVS observed an $\sim 70\%$ increase in the observed brightness of CO₂⁺ Ultraviolet Doublet and CO Cameron

⁴NASA Goddard Spaceflight Center,
Greenbelt, MD, USA

⁵Laboratoire de Physique Atmosphérique
et Planétaire, Space sciences (LPAP),
University of Liège, Liège, Belgium

⁶University of Arizona, Tucson, Arizona,
USA

⁷Center for Space Physics, Boston
University, Boston, Massachusetts

⁸LATMOS, CNRS, Guyancourt, France

band emission at 90 km, where high-energy photons (< 10 nm) deposit most of their energy.

Keypoints:

- Martian thermospheric temperatures increase by ~ 70 K in response to an X-class solar flare and returns to its normal value in next orbit (after ~ 4.5 hours).
- Dayglow emissions show significant enhancement below and above the airglow peak due to increased flux of soft x-ray and extreme ultraviolet photons.
- Thermospheric heating due to the flare was limited to low- and mid-latitudes

1. Introduction

The energetics of a planet's upper atmosphere are mainly governed by absorption of solar extreme ultraviolet (EUV) radiation [*Bougher and Roble, 1991; Bougher et al., 2017*].

Understanding the response of a planet's upper atmosphere to the daily, long and short-term variation in solar flux is important to quantify the energy budget of the upper atmosphere. Solar transient events, such as flares, can deposit large amount of energy in the atmosphere in a very short time ranging from a few minutes to a few hours, which results in rapid changes in the thermosphere and ionosphere [*Liu et al., 2007; Qian et al., 2011; Lollo et al., 2012; Mendillo et al., 2006*]. During a flare, the solar ionizing photon flux increases dramatically, resulting in excess ionization, dissociation, and heating of the atmospheres [*Liu et al., 2007; Qian et al., 2011*]. *Thiemann et al.* [2015] have recently reported the effect of solar flares on neutral densities and temperatures in the Martian thermosphere. *Thiemann et al.* [2015] have shown that the neutral atmospheric response to a flare is slightly delayed and long lived compared to that of the ionospheric response, which has a time profile similar to the flare [*Mendillo et al., 2006; Lollo et al., 2012; Haider et al., 2016*].

During a flare, the soft X-ray (SXR: 0.1–10 nm) irradiance can increase by two orders of magnitude [*Woods et al., 2004*]. These high energy photons are deposited in the lower thermosphere and are responsible for enhanced ionization in the ionospheric M1 layer at Mars [*Mendillo et al., 2006; Lollo et al., 2012*]. Increase in EUV irradiance can also lead to additional heating in the upper atmosphere. Solar EUV forcing is very important in controlling the Martian upper atmospheric temperatures [*Bougher et al., 2015, 2017*];

Jain et al., 2015]. Being the interface between the lower atmosphere and solar forcing from top, the upper atmosphere is the main reservoir for atmospheric escape to space and any variations in the temperature and density in the upper atmosphere affect escape rate [*Chaufray et al., 2015*]. Escape is recognized as a key driver of atmospheric change on Mars [e.g., *Lammer et al., 2008; Jakosky et al., 2015*], therefore a better characterization of upper atmospheric variability, including the effects of solar transient events, is a necessary step for a better understanding of the long-term atmospheric evolution of the planet.

In this letter, we report the response of the Martian upper atmosphere to a strong X-class flare on September 10, 2017 as observed by the Imaging Ultraviolet Spectrograph (IUVS) instrument aboard the Mars Atmosphere Volatile Evolution (MAVEN) mission. This event occurred when Mars was nearing aphelion ($L_s = 60^\circ$) and the nominal solar activity was quite low. This is the largest solar event observed by MAVEN since its orbit insertion in August 2014. The ionosphere and thermosphere of Mars showed a significant response to the flare, which was observed by multiple instruments onboard MAVEN [*Lee et al., 2018*]. We here report the first IUVS observations of Martian thermosphere temperature response to an X-class solar flare. The results presented in this letter will help us understand the role of solar transient events in the total heat budget of the Martian thermosphere. The following section explains the observations and methodology used in the analysis. The results of the IUVS dayglow analysis are presented in Section 3, followed by discussion and interpretation of the thermosphere response to the flare in Section 4. Concluding remarks are given in Section 5

2. Observation and Methodology

IUVS takes airglow limb measurements in the periapse segment of the MAVEN's orbit (orbital period ~ 4.5 hours) using its two detectors; a far ultraviolet (FUV) detector (115 - 190 nm) and a middle ultraviolet (MUV) detector (173 - 340 nm) with a spectral resolution of ~ 0.6 and 1.2 nm, respectively, [McClintock *et al.*, 2015]. IUVS takes twelve limb scans near periapsis (when the spacecraft altitude is below ~ 500 km) in about 40 minutes. The instrument is mounted on an Articulated Payload Platform (APP) that orients the IUVS' line of sight perpendicular to the spacecraft's motion and the projection of the slit onto the atmosphere is perpendicular to the planet's radial vector at slit center (see Figure 1). This causes IUVS limb observations, which are pointed normal to the spacecraft velocity vector, and in-situ measurements to observe completely different states of the Martian atmosphere (with different lighting, geometry, and local time). The details of IUVS dayglow limb observations have been provided previously [McClintock *et al.*, 2015; Jain *et al.*, 2015; Stevens *et al.*, 2015].

For the analysis presented in this paper, we use the CO_2^+ Ultraviolet Doublet (UVD) dayglow emission at 289 nm, which is one of the brightest MUV emissions in the Martian dayglow [Jain *et al.*, 2015; Leblanc *et al.*, 2006]. This emission is mainly produced by photon and electron impact ionization of CO_2 [Jain and Bhardwaj, 2012], making it an ideal diagnostic tool for retrieving information about the background neutral atmosphere [Jain *et al.*, 2015; Stiepen *et al.*, 2015; Evans *et al.*, 2015]. To retrieve scale heights and infer temperatures (at 170 km), we use an empirical Chapman fit to the CO_2^+ UVD emission intensity profile [Lo *et al.*, 2015; Bougher *et al.*, 2017]. We have imposed a maximum solar zenith angle constraint of 85° in our analysis of temperatures

(thus restricting observations to inbound scans only). We also omitted emission profiles from our analysis if the spacecraft altitude was below 200 km to avoid systematic lower temperatures when IUVS is observing from within the airglow layer.

IUVS limb scans of CO_2^+ UVD brightness are used to retrieve CO_2 density profiles using the approach described by *Evans et al.* [2015], with the exception of the treatment of solar EUV input to the forward model used for optimal estimation retrieval of densities.

When modeling the thermospheric response to solar flares, it is important to account for enhanced emission at lower altitudes due to short-term variability of the solar EUV and SXR irradiance, since insufficient solar input leads to incorrect enhancement in number density to account for increased emission. Therefore, we use minute cadence solar spectra and select the appropriate spectrum using the mean time of each IUVS limb scan.

The photons from the solar flare with a magnitude of 8.2 reached Mars on September 10, 2017, peaking near 16:24 UT. The nearest MAVEN periapsis occurred around 17:35 UT during orbit 5718, about one hour after the flare peaked. The IUVS line of sight (LOS) was pointing towards the dusk terminator at the time of dayglow measurements (see Figure 1) and observing at different local time (17:55 hrs local time) compared to the spacecraft (16:50 hrs local time) for the same 17:35 UT time. Due to the atypical nature of this event, we have used a solar spectrum (1 nm resolution) estimated at Mars by combining measurements from MAVEN's Extreme Ultraviolet Monitor (EUVM) and earth-based observations [please see *Thiemann et al.*, 2018, for more details]. At the time of the event, the MAVEN periapsis was on the dusk terminator in the Northern

hemisphere (see Figure 1) and the spacecraft was moving from low latitudes towards high latitudes.

3. Results

Figure 2 shows mean altitude profiles of CO_2^+ UVD brightness from orbits 5717 and 5719, before and after the flare (black curves), and from orbit 5718 during the peak of the flare (red curve) at a mean latitude of ~ 20 degrees during the inbound segment of MAVEN's periapsis. The ratio of intensities from non-flare orbits (mean of combined UVD intensities from orbits 5717 and 5719) and the flare orbit is also shown in the same panel. The dayglow emission was enhanced at all altitudes during the flare orbit.

Specifically, the intensity of CO_2^+ UVD increased by $\sim 70\%$ at 90 km, where most of the high energy photons (< 10 nm) are deposited. Above the airglow peak, the UVD emission from the flare orbit also shows enhanced brightness, with in the intensity with altitude (increasing two-fold at 180 km). The densities of retrieved neutral CO_2 from the flare and non-flare orbits are shown in Figure 2 (right panel) along with the corresponding density ratio. The shape of the flare orbit density profile indicates a higher scale height compared to non-flare orbits, which is consistent with the shape of the flare orbit UVD intensity profile. The maximum difference between flare and non-flare densities occurs at higher altitudes; at 190 km, the flare orbit CO_2 density is about a factor of 1.6 higher than during the non-flare orbits.

Temperatures derived from CO_2^+ UVD intensities spanning more than 100 orbits (7 September 2017 to 25 September 2017) are presented in Figure 3. The temperatures are averaged over a mean latitude of 20° . The mean temperature for all non-flare orbits is

~ 197 K, with a standard deviation of ± 18 K. The temperature for the flare observation is shown as a red symbol, which is a ~ 70 K higher than the mean. IUVS observed the higher temperatures only during the flare orbit, with no effect seen during the succeeding orbit 4.5 hrs later. An inset figure with temperatures retrieved on September 9 and 10, along with EUVM ionizing irradiation (total irradiance between 0 and 91 nm), is also shown in Figure 3. As mentioned earlier, the nearest IUVS observation to the solar flare peak occurred about one hour later, when the ionizing photon flux dropped nearly 80% from its maximum value.

Figure 4 shows the latitudinal behavior of the retrieved temperature between September 7 and 13, (orbits 5700 to 5730). Due to the slow precession of MAVEN's orbit, the latitude coverage before and after the flare was quite similar. Similarly, the lighting conditions (solar zenith angles, local time) do not vary much from orbit to orbit. This makes it easier to quantify the latitudinal variation of thermospheric temperatures, since other controlling factors are essentially constant with time. Under non-flare conditions, temperatures typically show a strong gradient with latitude, with larger temperatures at low latitudes (around 10°) and smaller values near mid latitudes ($\sim 30^\circ$). The temperatures retrieved during the flare orbit exhibit a similar latitudinal behavior. However, the temperature gradient is stronger during the flare orbit (-5.5 ± 0.2 K/deg) compared to the non-flare orbits (-1.9 ± 0.3 K/deg). Since each latitude observation is mapped to a certain time, we could compare the EUV ionizing irradiance measurements taken at that time, which are shown in Figure 4 for the flare orbit of 5718. The EUV ionizing radiance didn't show much decline ($< 2\%$), when IUVS took observation during the inbound periapse segment.

4. Discussion

The photon energy deposition rate changes significantly during the flare orbit. Model calculations by *Thiemann et al.* [2018] showed that during the flare peak, the photon energy deposition rate increased by 80-90% below 120 km, where most of the SXR photons deposit their energy, which causes the total photoionization rate to increase by almost 500% at these altitudes. At 160 km, the total ionization rate increased by about $\sim 20\%$ at the time of peak flare activity [*Thiemann et al.*, 2018]. We observed an enhanced CO_2^+ UVD emission below the airglow peak, where the UVD intensities increased by $\sim 70\%$ at 90 km (Figure 2). In the upper atmosphere, the elevated UVD intensity is due to increased ionization from EUV fluxes during the flare. However, the shape of the topside emission is representative of the neutral scale height, which is seen in the retrieved densities of neutral CO_2 . The neutral density shown in Figure 2 indicates that during the flare, the upper atmosphere was heated by enhanced EUV irradiation, which produced an increase in densities at higher altitudes. It is worth noting that increased UVD brightness at lower altitudes (~ 90 km) is due entirely to increased SXR photon irradiance during the flare rather than flare-induced perturbations in the CO_2 density (indeed, the flare orbit CO_2 density decreased relative to non-flare orbits).

Thiemann et al. [2015] investigated the effect of a solar flare on the Martian upper atmosphere temperatures and showed that the neutral upper atmosphere responds quickly to the flare, followed by a rapid recovery. IUVS retrieved temperatures in Figure 3 show a quick response of the Martian upper atmosphere to the X8.2 solar flare of 10 September 2017. Temperatures during flare orbit 5718 increased by ~ 70 K relative to the mean

temperature, and returned to nominal values in the following orbit 4.5 hrs later. Similarly, a rapid response (about an hour) to the effect of flares on terrestrial upper atmosphere densities (e.g., 400 km) has also been reported by *Sutton et al.* [2006]; *Liu et al.* [2007]; *Strickland et al.* [2007]; *Pawlowski and Ridley* [2008]. However, the terrestrial thermosphere densities takes hours to recover to their prior quiescent levels; *Sutton et al.* [2006] have reported recovery time of 12 hours for two X17 flares. The thermospheric temperatures of Mars is mainly controlled by the EUV heating and three main cooling mechanisms (molecular conduction, upwelling/divergent winds, and CO₂ 15- μ m cooling) [*Bougher et al.*, 1999]. The time constants for temperature relaxation following a flare may well be smaller for the Mars upper thermosphere owing to these 3-contributors to the cooling. A detailed model study to understand the response and recovery of Mars thermospheric temperatures to the flare event is beyond the scope of this paper and will be carried out in future.

The amount of heating of the upper atmosphere due to the flare depends on the corresponding spectral content, especially at EUV wavelengths [*Qian et al.*, 2010; *Le et al.*, 2012; *Thiemann et al.*, 2015]. During the September event, the EUV content of the flare's spectrum increased by 60% during its peak, but had decreased to about 16% at the time IUVS observed the airglow 4.5 hrs later. Thus, it is difficult to assess the quantitative effect of flare EUV flux on the thermosphere. However, based on studies of EUV forcing in Mars' upper atmosphere [*Bougher et al.*, 1999, 2015; *González-Galindo et al.*, 2005], it may be possible that IUVS observations of large temperature increases during the flare

orbit are caused by integrated energy deposited by the flare rather than energy deposited at the time of observations.

MAVEN's Neutral Gas and Ion Mass Spectrometer (NGIMS) also reported a neutral atmospheric response to the solar flare of 10 September 2017 [Elrod *et al.*, 2018]. NGIMS measurements showed enhanced neutral densities above 200 km and significantly larger temperatures only at high altitudes (>185 km), though NGIMS sampled slightly lower solar zenith angles compared to values at IUVS tangent points. NGIMS in-situ measurements are taken at the spacecraft altitude and latitude (see Figure 1). The spacecraft altitude is higher at lower latitudes and decreases with increasing latitude until MAVEN reaches periapsis. NGIMS probed the atmosphere below 200 km only near $\sim 30^\circ$ latitude, where IUVS retrieved temperatures during the flare orbit decreased significantly from the maximum value and were comparable to non-flare temperatures (please see Figure 4), which is consistent with an absence of any flare effects in NGIMS measurements below 200 km.

The latitude dependence of temperatures from the flare orbit is quite interesting, because it shows that the majority of the upper atmospheric heating due to the flare is confined to near the subsolar latitudes. The maximum difference between the retrieved temperature during the flare orbit and non-flare orbits has been observed near 10° latitude and the minimum difference was observed near the subsolar latitudes (between 20° and 30°). The solar EUV ionizing radiance didn't vary much during the inbound segment of orbit 5718 (flare orbit), ruling out the possible role of EUV to cause this decline in thermosphere temperature (see Figure 4). Terrestrial thermospheric density and temper-

atures also show latitudinal gradient during the flare, which follow cosine of solar zenith angle (SZA) [*Pawlowski and Ridley, 2008; Qian et al., 2011*]. However, during IUVS observations, the solar zenith angle was decreasing during the first half of the MAVEN periapse (the SZA was 87° at first scan and 76° at the periapsis). The temperatures at non-flare orbits also show similar latitudinal gradients (though not as strong as the flare orbit). This seems to suggest that the upper atmosphere dynamics may have played an important role in low-mid latitude temperature gradients observed by IUVS. Understanding this behavior requires further analysis and modeling, which will be the subject of a subsequent paper.

5. Summary and Conclusion

In this letter, we report the response of the Martian upper atmosphere to a strong X-class flare on September 10, 2017. Temperatures derived from IUVS observations during the flare orbit increased by $\sim 70\text{K}$, with a rapid recovery to non-flare values in the following orbit 4.5 hrs later. This suggests that the upper atmospheric response to the flare and subsequent recovery were both fast (within 4.5 hours of MAVEN orbit). Retrieved CO_2 densities also show an enhancement during the flare, particularly at higher altitudes, where the density increased by $\sim 60\%$. The upper atmospheric enhancements in temperature and density reflect a rapid response to the increased EUV irradiance during the flare, consistent with our understanding of these events. The CO_2^+ UVD intensity below the airglow peak increased by a factor of 1.6 following the peak of the flare due to deposition of high energy SXR photons below ~ 120 km.

This event provides a unique opportunity to study the response of Mars' upper atmosphere to an extreme X-class solar flare. Such observational studies on Mars are quite rare due to the low occurrence rate of X-class flares. However, they are crucial for improving our understanding of the energy budget of the Martian upper atmosphere and the long-term evolution and escape of the Martian atmosphere. Within the limits of our observing geometry and lighting conditions, such as latitude and local time, this study provides an important constraint on upper atmospheric parameters (temperature, density) during an extreme solar transient event which can be compared to models in future studies.

Acknowledgments. The MAVEN mission is supported by NASA in association with the University of Colorado and NASA's Goddard Space Flight Center. The level 1C data used in this analysis are archived (tagged "periapse" with version/revision tag v12_r01) in NASA's Planetary Data System (PDS), http://atmos.nmsu.edu/data_and_services/atmospheres_data/MAVEN/maven_iuvs.html.

References

- Bougher, S. W., and R. G. Roble (1991), Comparative terrestrial planet thermospheres: 1. solar cycle variation of global mean temperatures, *Journal of Geophysical Research: Space Physics*, *96*(A7), 11,045–11,055, doi:10.1029/91JA01162.
- Bougher, S. W., S. Engel, R. G. Roble, and B. Foster (1999), Comparative terrestrial planet thermospheres: 2. Solar cycle variation of global structure and winds at equinox, *J. Geophys. Res.*, *104*, 16,591 – 16,611, doi:10.1029/1998JE001019.

Bougher, S. W., D. Pawlowski, J. M. Bell, S. Nelli, T. McDunn, J. R. Murphy, M. Chizek, and A. Ridley (2015), Mars global ionosphere-thermosphere model: Solar cycle, seasonal, and diurnal variations of the mars upper atmosphere, *J. Geophys. Res.*, *120*(2), 311–342, doi:10.1002/2014JE004715, 2014JE004715.

Bougher, S. W., D. A. Brain, J. L. Fox, G.-G. Francisco, C. Simon-Wedlund, and P. G. Withers (2017), Upper Neutral Atmosphere and Ionosphere, in *The atmosphere and climate of Mars*, edited by R. M. Haberle, R. T. Clancy, F. Forget, M. D. Smith, and R. W. Zurek, pp. 405–432, Cambridge University Press, doi:10.1017/9781139060172.014.

Bougher, S. W., K. J. Roeten, K. Olsen, P. R. Mahaffy, M. Benna, M. Elrod, S. K. Jain, N. M. Schneider, J. Deighan, E. Thiemann, F. G. Eparvier, A. Stiepen, and B. M. Jakosky (2017), The structure and variability of mars dayside thermosphere from MAVEN NGIMS and IUVS measurements: Seasonal and solar activity trends in scale heights and temperatures, *J Geophys Res Space Phys*, *122*(1), 1296–1313, doi:10.1002/2016ja023454.

Chaufray, J., G. F. Forget, L. M.A., F. Leblanc, R. Modolo, and S. Hess (2015), Variability of the hydrogen in the martian upper atmosphere as simulated by a 3D atmosphere-exosphere coupling, *Icarus*, *245*, 282–294, doi:10.1016/j.icarus.2014.08.038.

Elrod, M., E. M. B. Thiemann, S. Curry, and J. S. K. (2018), September 2017 Solar Flare Event: Rapid Heating of the Martian Neutral Exosphere from the X-class flare as observed by MAVEN, *Geophys. Res. Lett.*, this issue: 2018GL077729.

Evans, J. S., M. H. Stevens, J. D. Lumpe, N. M. Schneider, A. I. F. Stewart, J. Deighan, S. K. Jain, M. S. Chaffin, M. Crismani, A. Stiepen, W. E. McClintock, G. M. Holsclaw, F. Lefèvre, D. Y. Lo, J. T. Clarke, F. Eparvier, E. M. B. Thiemann, F. Montmessin, and B. M. Jakosky (2015), Retrieval of CO₂ and N₂ in the Martian thermosphere using dayglow observations by IUVS on MAVEN, *Geophys. Res. Lett.*, *42*, 9040–9049, doi:10.1002/2015GL065489.

González-Galindo, F., M. A. Lopez-Valverde, M. Angelats i Coll, and F. Forget (2005), Extension of a martian general circulation model to thermospheric altitudes: Uv heating and photochemical models, *J. Geophys. Res.*, *110*(E9), 2156–2202, doi:10.1029/2004JE002312, e09008.

Haider, S. A., I. S. Batista, M. Abdu, A. M. Santos, S. Y. Shah, and P. Thirupathaiah (2016), Flare x-ray photochemistry of the e region ionosphere of mars, *J. Geophys. Res.*, *121*(7), 6870–6888, doi:10.1002/2016JA022435, 2016JA022435.

Jain, S. K., and A. Bhardwaj (2012), Impact of solar EUV flux on CO Cameron band and CO₂⁺ UV doublet emissions in the dayglow of Mars, *Planet. Space Sci.*, *63-64*, 110–122, doi:10.1016/j.pss.2011.08.010.

Jain, S. K., A. I. F. Stewart, N. M. Schneider, J. Deighan, A. Stiepen, J. S. Evans, M. H. Stevens, M. S. Chaffin, M. Crismani, W. E. McClintock, J. T. Clarke, G. M. Holsclaw, D. Y. Lo, F. Lefèvre, F. Montmessin, E. M. B. Thiemann, F. Eparvier, and B. M. Jakosky (2015), The structure and variability of Mars upper atmosphere as seen in MAVEN/IUVS dayglow observations, *Geophys. Res. Lett.*, *42*, 9023–9030, doi:10.1002/2015GL065419.

Jakosky, B. M., R. P. Lin, J. M. Grebowsky, J. G. Luhmann, D. F. Mitchell, G. Beutelschies, T. Priser, M. Acuna, L. Andersson, D. Baird, D. Baker, R. Bartlett, M. Benna, S. Bougher, D. Brain, D. Carson, S. Cauffman, P. Chamberlin, J.-Y. Chaufray, O. Cheatom, J. Clarke, J. Connerney, T. Cravens, D. Curtis, G. Delory, S. Demcak, A. DeWolfe, F. Eparvier, R. Ergun, A. Eriksson, J. Espley, X. Fang, D. Folta, J. Fox, C. Gomez-Rosa, S. Habenicht, J. Halekas, G. Holsclaw, M. Houghton, R. Howard, M. Jarosz, N. Jedrich, M. Johnson, W. Kasprzak, M. Kelley, T. King, M. Lankton, D. Larson, F. Leblanc, F. Lefevre, R. Lillis, P. Mahaffy, C. Mazelle, W. McClintock, J. McFadden, D. L. Mitchell, F. Montmessin, J. Morrissey, W. Peterson, W. Possel, J.-A. Sauvaud, N. Schneider, W. Sidney, S. Sparacino, A. I. F. Stewart, R. Tolson, D. Toubanc, C. Waters, T. Woods, R. Yelle, and R. Zurek (2015), The Mars Atmosphere and Volatile Evolution (MAVEN) Mission, *Space Sci. Rev.*, *195*, 3–48, doi:10.1007/s11214-015-0139-x.

Lammer, H., J. F. Kasting, E. Chassefière, R. E. Johnson, Y. N. Kulikov, and F. Tian (2008), Atmospheric escape and evolution of terrestrial planets and satellites, *Space Sci. Rev.*, *139*(1-4), 399–436, doi:10.1007/s11214-008-9413-5.

Le, H., L. Liu, and W. Wan (2012), An analysis of thermospheric density response to solar flares during 20012006, *J. Geophys. Res.*, *117*(A3), 2156–2202, doi:10.1029/2011JA017214, a03307.

Leblanc, F., J. Y. Chaufray, J. Lilensten, O. Witasse, and J.-L. Bertaux (2006), Martian dayglow as seen by the SPICAM UV spectrograph on Mars Express, *J. Geophys. Res.*, *111*, E09S11, doi:10.1029/2005JE002664.

- Lee, C. et al. (2018), Observations and Impacts of the 10 September 2017 Solar Events at Mars: An Overview and Synthesis of the Initial Results, *Geophys. Res. Lett.*, this issue.
- Liu, H., H. Lühr, S. Watanabe, W. Köhler, and C. Manoj (2007), Contrasting behavior of the thermosphere and ionosphere in response to the 28 October 2003 solar flare, *J. Geophys. Res.*, *112*, A07305, doi:10.1029/2007JA012313.
- Lo, D. Y., R. V. Yelle, N. M. Schneider, S. K. Jain, A. I. F. Stewart, S. England, J. Deighan, A. Stiepen, J. S. Evans, M. H. Stevens, M. S. Chaffin, M. Crismani, W. E. McClintock, J. T. Clarke, G. M. Holsclaw, and B. M. Jakosky (2015), Tides in the Martian Atmosphere as Observed by MAVEN IUVS, *Geophys. Res. Lett.*, *42*, 9057–9063, doi:10.1002/2015GL066268.
- Lollo, A., P. Withers, K. Fallows, Z. Girazian, M. Matta, and P. C. Chamberlin (2012), Numerical simulations of the ionosphere of mars during a solar flare, *J. Geophys. Res.*, *117*(A5), 2156–2202, doi:10.1029/2011JA017399, a05314.
- McClintock, W. E., N. M. Schneider, G. M. Holsclaw, J. T. Clarke, A. C. Hoskins, I. Stewart, F. Montmessin, R. V. Yelle, and J. Deighan (2015), The Imaging Ultraviolet Spectrograph (IUVS) for the MAVEN Mission, *Space Sci. Rev.*, *195*, 75–124, doi:10.1007/s11214-014-0098-7.
- Mendillo, M., P. Withers, D. Hinson, H. Rishbeth, and B. Reinisch (2006), Effects of Solar Flares on the Ionosphere of Mars, *Science*, *311*, 1135–1138, doi:10.1126/science.1122099.
- Pawlowski, D. J., and A. J. Ridley (2008), Modeling the thermospheric response to solar flares, *J. Geophys. Res.*, *113*, A10309, doi:10.1029/2008JA013182.

Qian, L., A. G. Burns, P. C. Chamberlin, and S. C. Solomon (2010), Flare location on the solar disk: Modeling the thermosphere and ionosphere response, *J. Geophys. Res.*, *115*(A9), 2156–2202, doi:10.1029/2009JA015225, a09311.

Qian, L., A. G. Burns, P. C. Chamberlin, and S. C. Solomon (2011), Variability of thermosphere and ionosphere responses to solar flares, *J. Geophys. Res.*, *116*(A10), 2156–2202, doi:10.1029/2011JA016777, a10309.

Stevens, M. H., J. S. Evans, N. M. Schneider, A. I. F. Stewart, J. Deighan, S. K. Jain, M. Crismani, A. Stiepen, M. S. Chaffin, W. E. McClintock, G. M. Holsclaw, F. Lefèvre, D. Y. Lo, J. T. Clarke, F. Montmessin, and B. M. Jakosky (2015), N₂ in the upper atmosphere of Mars observed by IUVS on MAVEN, *Geophys. Res. Lett.*, *42*, 9050–9056, doi:10.1002/2015GL065319.

Stiepen, A., J.-C. Gérard, S. Bougher, F. Montmessin, B. Hubert, and J.-L. Bertaux (2015), Mars thermospheric scale height: CO Cameron and CO₂⁺ dayglow observations from Mars Express, *Icarus*, *245*, 295–305, doi:10.1016/j.icarus.2014.09.051.

Strickland, D. J., J. L. Lean, R. E. Daniell, H. K. Knight, W. K. Woo, R. R. Meier, P. R. Straus, T. N. Woods, F. G. Eparvier, D. R. McMullin, A. B. Christensen, D. Morrison, and L. J. Paxton (2007), Constraining and validating the oct/nov 2003 x-class euv flare enhancements with observations of fuv dayglow and e-region electron densities, *Journal of Geophysical Research: Space Physics*, *112*(A6), 2156–2202, doi:10.1029/2006JA012074.

Sutton, E. K., J. M. Forbes, R. S. Nerem, and T. N. Woods (2006), Neutral density response to the solar flares of october and november, 2003, *Geophysical Research Letters*,

33(22), 1944–8007, doi:10.1029/2006GL027737, l22101.

Thiemann, E. M. B., F. G. Eparvier, L. A. Andersson, C. M. Fowler, W. K. Peterson, P. R. Mahaffy, S. L. England, D. E. Larson, D. Y. Lo, N. M. Schneider, J. I. Deighan, W. E. McClintock, and B. M. Jakosky (2015), Neutral density response to solar flares at Mars, *Geophys. Res. Lett.*, *42*, 8986–8992, doi:10.1002/2015GL066334.

Thiemann, E. M. B., L. A. Andersson, R. Lillis, P. Withers, S. Xu, M. Elrod, D. Pawlowski, P. C. Chamberlin, F. G. Eparvier, M. Benna, C. M. Fowler, M. D. Pilinski, and S. Curry (2018), The Mars Upper Ionosphere Response to the X8.2 Solar Flare of 10 September 2017, *Geophys. Res. Lett.*, this issue: 2018GL077730.

Woods, T. N., F. G. Eparvier, J. Fontenla, J. Harder, G. Kopp, W. E. McClintock, G. Rottman, B. Smiley, and M. Snow (2004), Solar irradiance variability during the october 2003 solar storm period, *Geophys. Res. Lett.*, *31*(10), 1944–8007, doi:10.1029/2004GL019571, 110802.

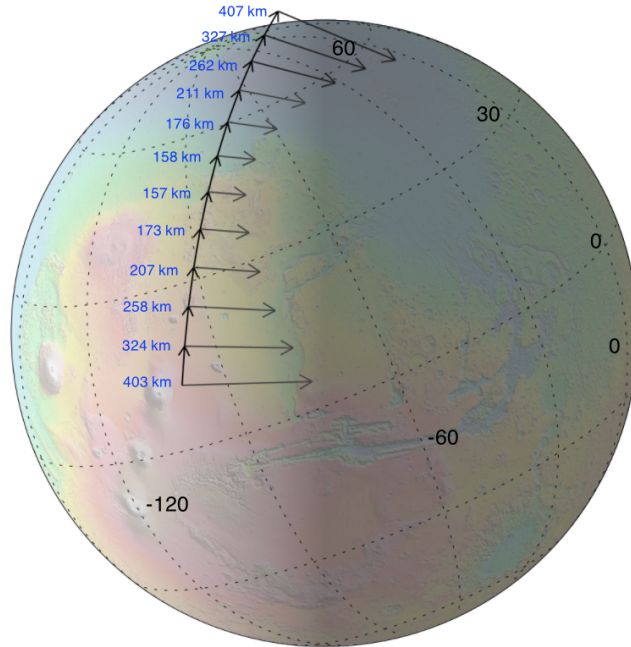


Figure 1. The MAVEN periape segment and IUVS observing geometry during flare orbit 5718 on September 10, 17:35 UT. The tails of the vertical velocity vectors indicate the locations of the sub-spacecraft latitude and longitude during twelve IUVS limb scans. The numbers next to the velocity vectors indicate spacecraft altitude. The horizontal arrows show the latitude and longitude of the IUVS tangent lines of sight. The altitude of IUVS LOS roughly spans between 80-220 km

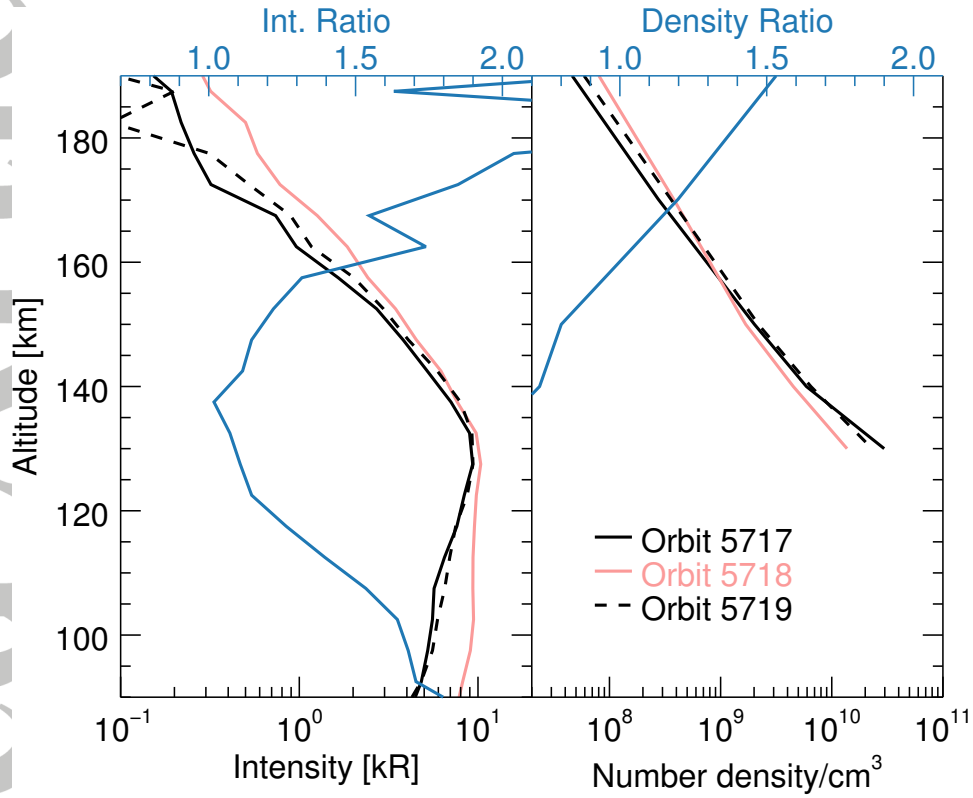


Figure 2. (left) CO₂⁺ UVD profiles for pre-flare (solid black), flare (red) and post-flare (dashed black) conditions. These profiles are the average of all inbound scans with resulting mean latitude of 20°. The ratio of flare (5718) and nominal orbits (mean of all inbound UVD profiles from 5717 and 5719) is shown in blue (top x-axis). (right) Same as left, but for the retrieved CO₂ densities.

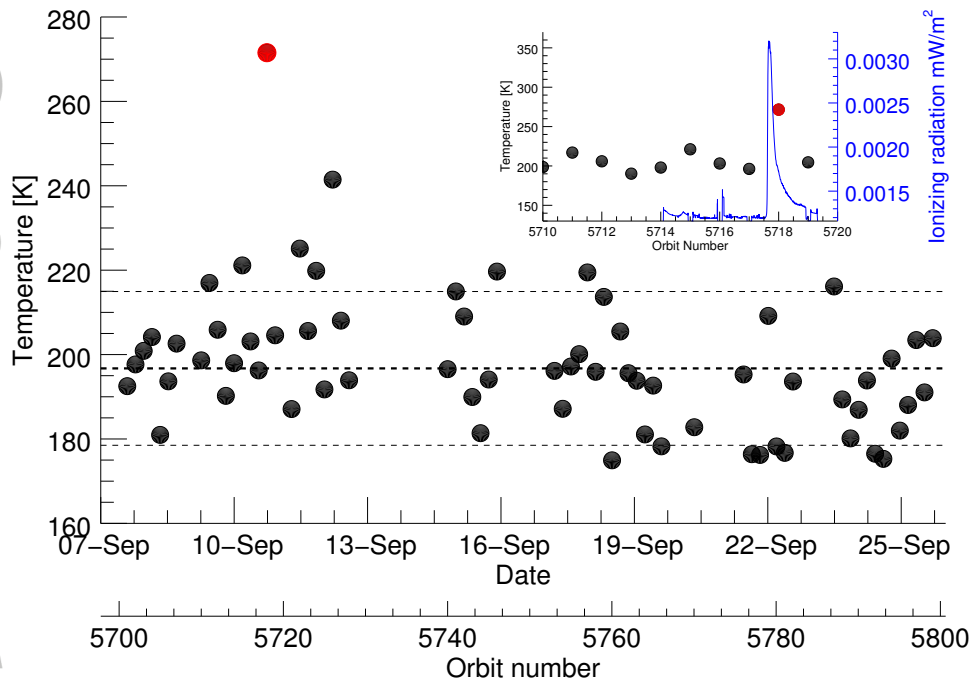


Figure 3. Temperatures derived from IUVS airglow measurements between 7 September and 25 September. The temperatures are averaged from all inbound scans for a mean latitude of $\sim 20^\circ$. The temperature for the flare orbit is shown as a red symbol. The thick and thin dashed curves show the mean and ± 1 standard deviation, respectively. The uncertainty in an individual temperature fit is quite small (± 2 K) compared to the standard deviation per orbit. A zoomed version is presented in the inset showing the temperature near flare orbit along with the total ionizing solar irradiance (0-91 nm) on the right y-axis.

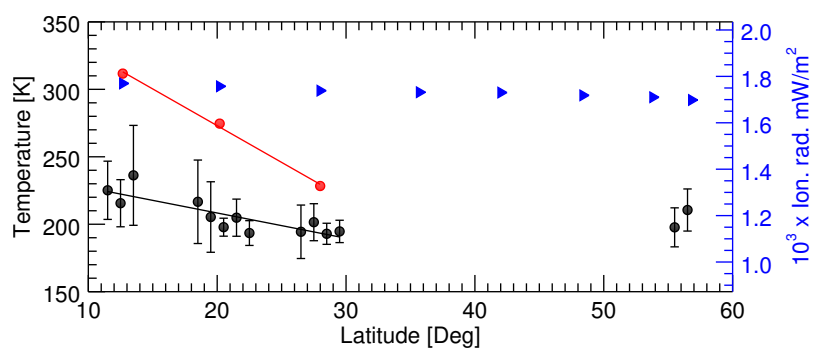


Figure 4. Retrieved temperatures from IUVS dayglow at different latitudes for all the profiles taken during September 7 and 13, 2017 (between orbits 5700 and 5730). The vertical black bars represent 1- σ standard deviation in the temperatures for given latitude bin. The values for the flare orbit are shown with red symbol. The mean SZA near 12, 20 and 28 degrees latitude is about 83°, 81°, and 78°, respectively. The black and red lines show the linear fit to the non-flare orbit and flare orbit temperatures (up to 30° latitude), with a slope of -5.5 ± 0.2 K/deg and -1.9 ± 0.3 K/deg, respectively. The blue symbols show the solar ionizing irradiance (0–91 nm; right y-axis) for the flare orbit taking into consideration the time for each latitude.